Nonlinear Panel Flutter by Finite-Element Method

B. S. Sarma*
Defence Research and Development Laboratory, Hyderabad, India
and
T. K. Varadan†
Indian Institute of Technology, Madras, India

The finite-element method is used here to study nonlinear panel flutter behavior. The governing nonlinear equations are derived from energy considerations, and the nonlinear stretching force is formulated in terms of the transverse displacement alone. Two solution approaches are adopted to solve the nonlinear panel flutter equations. In the first approach, the solution is obtained through the nonlinear vibration mode as the starting point, whereas in the second approach, it is obtained through the linear panel flutter mode as the starting point. The critical dynamic pressure for a given limit cycle amplitude is determined when the flutter frequency values of the first two modes coalesce. Aerodynamic damping is taken into account based on the two available simplifications, and a relation between these two simplifications is brought out. The panel behavior is analyzed from the response parameters of the complex eigenvalues. Numerical results are presented for all boundary conditions of the panel in the form of tables and graphs for different limit cycle amplitudes and are compared with the available analytical and finite-element solutions. Results based on the second solution approach are thought to be an improvement over those based on the first one, and they predict higher critical dynamic pressure values.

Introduction

LINEAR panel flutter analysis shows that there is a critical dynamic pressure value above which the panel motion becomes unstable and grows exponentially with time, whereas the inclusion of geometric nonlinear terms in the analysis makes the panel motion generally restrained and bounded into a limit cycle oscillation. Dowell[1] reviewed the work done on linear panel flutter, and Dugundji[2] presented the theoretical considerations of linear panel flutter. Various analytical techniques have been used to study nonlinear panel flutter behavior.[3-10] In all these studies, the Galerkin method with the assumed mode shape has been used, and different methods like direct numerical integration, perturbation, and the harmonic balance method have been adopted to solve the resulting equations of motion.

Olson[11] and Sanders[12] have successfully used the finite-element method to study linear panel flutter behavior. Chuh Mei,[13] Chuh Mei and Rogers,[14] and Rao et al.[15] have used the equivalent linearization technique in the finite-element formulations of nonlinear panel flutter. Prathap[16] made a comment on satisfying the immovable edge conditions at the element level instead of at the system level in the earlier work.[13] The present authors[17] have discussed the various approximations that have resulted in the formulations of nonlinear vibrations by the finite-element method.[13-15]

In the present work, the governing equations for nonlinear panel flutter by the finite-element method are derived from energy considerations by using Lagrange's equations of motion without any approximations on nonlinear terms pertaining to moderately large oscillations. Specifying the properties of time function at the point of motion reversal for an undamped case, the governing equations are reduced to nonlinear algebraic equations and are solved as a double-eigenvalue problem with appropriate nondimensionalization for the frequency parameter as well as the dynamic pressure. Two solution approaches have been used to get the frequency values for a given dynamic pressure at a specified amplitude value. In the first approach, the nonlinear vibration problem is solved iteratively for a given amplitude value and the nonlinear flutter solution is obtained by adding the aerodynamic force matrix of the corresponding dynamic pressure value.[3,6,7] In the second approach, the nonlinear panel flutter solution at a given amplitude value is obtained for a dynamic pressure value by iterating the linear panel flutter solution with the updated nonlinear stretching force in each iteration.[13-15] The critical dynamic pressure value is obtained by using the frequency coalescence condition. The nonlinear stretching forces obtained by the two methods have been different, as expected. In both cases, the effect of aerodynamic damping on the critical dynamic pressure value for the amplitude values considered has been evaluated from the response parameters of the complex eigenvalue.

Numerical results for critical dynamic pressure for various amplitude values are presented for hinged-hinged, clamped-clamped, clamped-hinged, and hinged-clamped panels. The change of mode shapes with dynamic pressure and the change of nonlinear stretching force in both solution approaches have been presented for a hinged-hinged panel at a specified amplitude value. Comparisons are made to the available results wherever possible, and the present results show a good agreement in the case of linear panel flutter and from the first approach for nonlinear panel flutter.

Governing Equations

The panel is represented by a flat plate of unit width with the airstream flowing over the upper surface in the positive direction of x, as shown in Fig. 1, and the effect of air in the lower surfaces is neglected. The strain-displacement relation with u as the axial displacement and w as the transverse displacement is written as

$$\epsilon_x = u_{,x} + \tfrac{1}{2} w_{,x}^2 - z w_{,xx} \tag{1}$$

where ( ), x represents the derivative of ( ) with respect to x. The strain energy U of the panel[19,20] (isotropic) is written as

$$U = \frac{EI}{2}\int_0^L w_{,xx}^2 \mathrm{d}x + \frac{EA}{2}\int_0^L (u_{,x} + \tfrac{1}{2} w_{,x}^2)^2 \mathrm{d}x \tag{2}$$

Received Aug. 11, 1986; revision received April 2, 1987.

*Scientist.

†Professor, Department of Aeronautical Engineering.

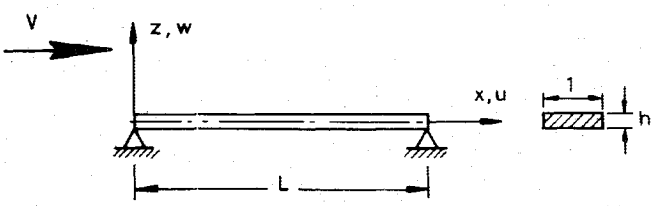

Fig. 1 Panel geometry.

where E is the modulus of elasticity, L is the length of the panel, and I and A are the moment of inertia and the area of the cross section, respectively. The kinetic energy T of the panel is written as

$$T=\frac{m}{2}\int_0^L (\dot{u}^2+\dot{w}^2)\mathrm{d}x \tag{3}$$

where m is the mass per unit length of the panel and ($\dot{}$) denotes the derivative of ( ) with respect to time. The virtual work V of the aerodynamic forces is written as[11]

$$V=Q_i q_i=\int_{\text{Surf}} \Delta p(x,y,t)\, w \,\text{dsurf} \tag{4}$$

The aerodynamic pressure $\Delta p(x,y,t)$ for a sufficiently high Mach number ($M_\infty > 1.6$) can be suitably described by Quasisteady Supersonic flow theory[11,18] as

$$\Delta p(x,y,t)=\left(\frac{-2q}{\sqrt{M_\infty^2-1}}\right)\left[\frac{\partial w}{\partial x}+\frac{1}{V_a}\left(\frac{M_\infty^2-2}{M_\infty^2-1}\right)\frac{\partial w}{\partial t}\right] \tag{5}$$

where q is the dynamic pressure, M_∞ is the Mach number, and V_a is the velocity of airstream.

The Lagrange's equations of motion along the x and z directions are written as

$$\frac{\mathrm{d}}{\mathrm{d}t}\left(\frac{\partial T}{\partial \dot{u}_i}\right)+\left(\frac{\partial U}{\partial u_i}\right)=0$$
$$\frac{\mathrm{d}}{\mathrm{d}t}\left(\frac{\partial T}{\partial \dot{w}_i}\right)+\left(\frac{\partial U}{\partial w_i}\right)=Q_i \tag{6}$$

Following the simplification procedure adopted by the authors,[19] the governing equations are formulated in terms of the transverse displacement w and are written in the matrix form with proper nondimensionalization as

$$[M]\{\ddot{w}_i\}+\{[K_L]+N_x[K_{NL}]\}\{w_i\}+\lambda[A]\{w_i\}$$
$$+g_a[M]\{\dot{w}_i\}=0 \tag{7}$$

and

$$N_x=\frac{EA}{2}\int_0^L w_{,x}^2\mathrm{d}x=\frac{EA}{2L}\{w_i\}^T[K_{NL}]\{w_i\} \tag{8}$$

where $[M]$ is the consistent mass matrix, $[K_L]$ is the linear stiffness matrix, $[K_{NL}]$ is the nonlinear stiffness matrix, $[A]$ is the aerodynamic coefficients matrix, λ is the nondimensionalized aerodynamic pressure, $\lambda=2qL^3/\beta D$ where $\beta=\sqrt{M_\infty^2-1}$ and D is the bending stiffness of the panel ($Et^3/12$), and g_a is the nondimensionalized aerodynamic damping coefficient $\{(2q/\beta^3 D)(M_\infty^2-2/V_a)L^3\}$.

The properties of time function at the point of reversal of motion[19,20] for an undamped case, i.e., when $g_a=0$, are defined as $\{\ddot{w}_i\}_{\max}=k\{w_i\}_{\max}$, where $k=-(\Omega/\omega_0)^2$ in which $\omega_0^2=(D/mL^4)$ and Ω is a complex parameter written as $(\alpha+i\omega)$. The stability of the system is characterized from the response parameters α and ω where α is the damping factor. The governing nonlinear algebraic equations will then be written as

$$\{[K_L]+N_x[K_{NL}]+\lambda[A]-k[M]\}\{w_i\}_{\max}=0 \tag{9}$$

Element Representation

A two-noded beam element with four degrees of freedom per node is chosen in the present analysis. The performance of this element is seen to be excellent in the case of nonlinear vibrations of beams[19,20] and requires just four elements in a half-beam to achieve good convergence for frequency values for a hinged-hinged beam.[19] Figure 2 shows the element coordinates and degrees of freedom at each node. The transverse displacement $w(x)$ is represented by a seventh-order polynomial in x as

$$w(x)=[A(x)]\{a_i\} \tag{10}$$

where

$$A(x)=[1\ x\ x^2\ x^3\ x^4\ x^5\ x^6\ x^7]$$

and

$$\{a_i\}^T=[a_1\ a_2\ a_3\ a_4\ a_5\ a_6\ a_7\ a_8]$$

The element stiffness matrix $[K_L]_e$, the consistent mass matrix $[M]_e$, and the nonlinear stiffness matrix $[K_{NL}]_e$ are derived in Ref. 19. The element aerodynamic coefficients matrix $[A]_e$ is written as

$$[A]_e=[\Gamma]^T\int_0^\ell [A(x)^t A(x)_{,x}]\mathrm{d}x[\Gamma] \tag{11}$$

where $[\Gamma]$ is the transformation matrix as given in Ref. 19. A standard assembly procedure is adopted to assemble the element stiffness matrix, mass matrix, and aerodynamic coefficients matrix.

Solution

Equation (9) degenerates to that corresponding to the nonlinear vibration problem in vacuo when $\lambda=0$ and to that of a linear panel flutter problem when $N_x=0$. Equation (9) results in an eigenvalue problem in which the eigenvalues k_i are obtained for a given value of aerodynamic pressure λ. While the matrices $[K]$, $[K_{NL}]$, and $[M]$ are real and positive definite, $[A]$ is a semipositive definite matrix. With the increase in the value of λ in Eq. (9), the two natural frequencies coalesce to k_{cr} at a value $\lambda=\lambda_{cr}$ and then become a complex conjugate pair for any value of $\lambda>\lambda_{cr}$, i.e., $k=k_R\pm ik_I$ for $\lambda>\lambda_{cr}$. Hence, the stability criteria adopted here is that the critical dynamic pressure λ_{cr} is considered to be the lowest value of λ at which coalescence occurs among all values of limit cycle amplitudes corresponding to the linear case ($a=0$). In the absence of aerodynamic damping,

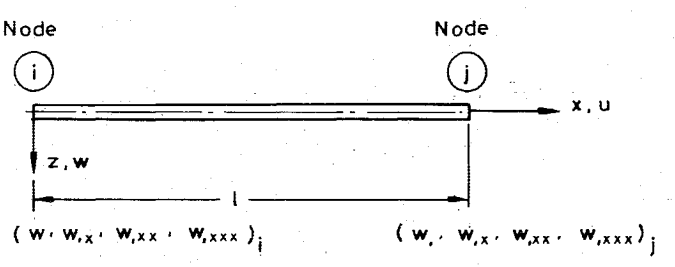

Fig. 2 Element nodal displacements.

the flutter boundary corresponds to λ_{cr}. When aerodynamic damping is considered, the value of λ_{cr} increases, and the extent of its increase is calculated from the panel response parameters, described later in detail. When $\lambda<\lambda_{cr}$, any disturbance to the panel decays, and the amplitude tends to zero. For $\lambda>\lambda_{cr}$, a limit cycle oscillation exists, and the amplitude increases as λ increases. The solution to the governing Eq. (9) is considered here in two ways.

First Approach

Initially, Eq. (9) is solved for the nonlinear vibration problem by making $\lambda=0$ for a given reference amplitude (a/h). The convergence of this solution vector is checked by using all three convergence norms of Ref. 21 and the frequency norm[13] for the frequency parameter. As λ is increased from zero, the resulting matrices have real and complex eigenvalues k. The critical dynamic pressure λ_{cr} is obtained by finding the lowest value of λ at which a pair of complex conjugate eigenvalues for k appear. This procedure of finding λ_{cr} is much the same as that of linear panel flutter, and the nonlinear problem is solved through a nonlinear vibration solution. The same approach is also used in Refs. 3, 6, and 7, whereas the nonlinear stretching force N_x is evaluated using a linear mode shape for a hinged-hinged panel without the effect of dynamic pressure (i.e., $\lambda=0$), and the resulting equations are solved for nonlinear panel flutter using a numerical integration technique,[3] perturbation technique,[6,7] and harmonic balance method.[7] If one looks carefully in the past investigations of nonlinear vibrations of one-dimensional problems, it can be noted that the mode shapes of both linear and nonlinear vibrations are the same for a hinged-hinged panel. However, for all other boundary conditions, the mode shape changes with the change in the amplitude value.

The aerodynamic damping is simplified as a nondimensional quantity (μ/M_∞)[3-7] where $\mu=(\rho L/\rho_a h)$ in which ρ is the material density, ρ_a is the air density, and M_∞ is the Mach number. In Ref. 22 it is shown that the aerodynamic damping value (μ/M_∞) can be obtained from the response parameters k_R and K_I of the panel along with the stability criteria of Houbolt and Movchan,[2,18] and it is written as

$$(\mu/M_\infty)=(1/\lambda)(k_I^2/k_R) \tag{12}$$

A typical case of amplitude by thickness value of 0.6 is considered to demonstrate the first approach, and two eigenvalues k_1 and k_2 for different λ values are plotted in Fig. 3, referred to as case a. The coalescence of k_1 and k_2 has taken place as λ is increased to λ_{cr} and for $\lambda>\lambda_{cr}$; k has become a complex conjugate pair. The aerodynamic damping parameter (μ/M_∞) is calculated from k_R and k_I values using Eq. (12) and is plotted in Fig. 4. One can notice from this figure that the aerodynamic damping is linearly dependent on the dynamic pressure λ and λ_{cr} has increased with the increase in (μ/M_∞) as observed in Refs. 3 and 6.

Second Approach

The standing wave-type mode shape for $\lambda=0$ changes into a traveling wave-type for $\lambda\geq\lambda_{cr}$ for linear panel flutter.[2] In the first approach, the nonlinear stretching force N_x is calculated on a standing wave-type mode (when $\lambda=0$), and it is taken to be constant in the nonlinear flutter analysis also. This results in a reduced hardening behavior in the case of nonlinear panel flutter. To account for the effect of dynamic pressure λ on the nonlinear stretching force N_x because of change of mode shape and hence nonlinear panel behavior, a second approach is considered here. The solution procedure outlined next is similar to those given in Refs. 13-15.

For a given λ value, the linear panel flutter equation obtained by making $N_x=0$ in Eq. (9) as

$$k[M]\{w_i\}_0=([K]+\lambda[A])\{w_i\}_0 \tag{13}$$

is solved. The linear flutter mode shape $\{w_i\}_0$ is normalized by its maximum value, and the starting mode shape for nonlinear panel flutter is taken as $(a/h)\{w_i\}_0$, where (a/h) is the reference amplitude value. The nonlinear stretching force N_x is calculated from Eq. (8) as

$$N_{x0}=\frac{EA}{2L}\{w_i\}_0^T[K_{NL}]\{w_i\}_0 \tag{14}$$

Equation (9) is written, for the ith iteration, as

$$k_i[M]\{w_i\}_i=\{[K]+N_x[K_{NL}]+\lambda[A]\}\{w_i\}_i \tag{15}$$

where k_i is the eigenvalue associated with the amplitude (a/h) and $\{w_i\}_i$ is the mode shape during the ith iteration. This iterative procedure is repeated until all three convergence norms on mode shapes[19,21] and the frequency norm

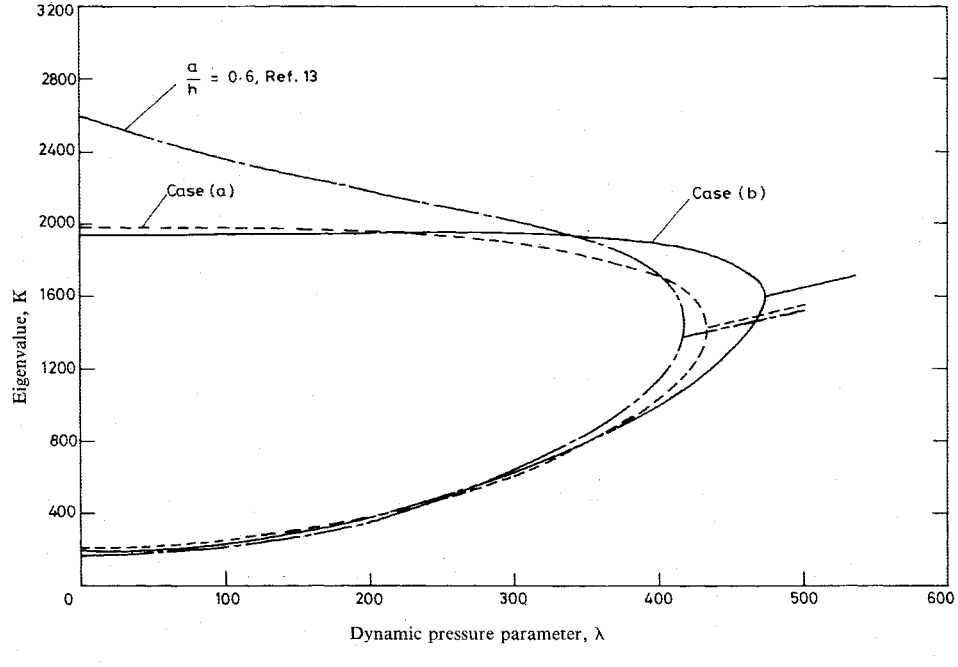

Fig. 3 Typical plot showing the variation of eigenvalues with dynamic pressure, hinged-hinged panel; $(a/h)=0.6$.

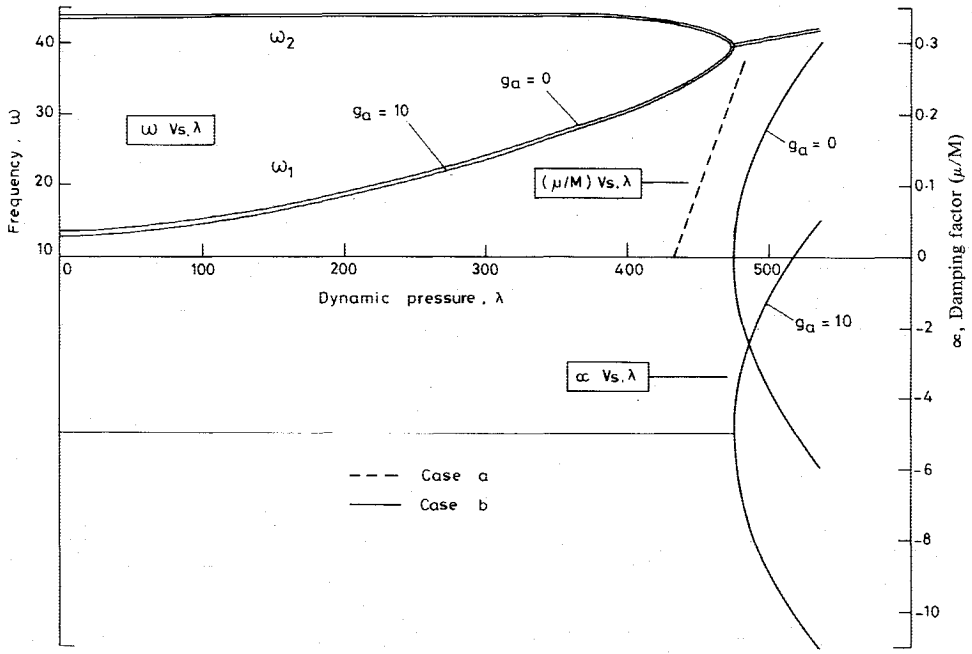

Fig. 4 Typical plot of response parameters α, ω, and μ/M_∞ against dynamic pressure, hinged-hinged panel; $(a/h) = 0.6$.

on the eigenvalue parameter[13] are satisfied for a given epsilon value ($\epsilon = 10^{-3}$). The stability criteria adopted in this case is exactly the same as that of the first approach. The lowest value of λ for which coalescence occurs for a specified limit cycle amplitude corresponds to the case when aerodynamic damping $g_a = 0.0$.

When the aerodynamic damping g_a is considered (g_a can also be total damping, which also includes velocity-type structural damping),[2] the eigenvalue with a negative imaginary part leads to instability,[12,13] and it is defined as

$$k = k_R - ik_I = -\left[\left(\frac{\Omega}{\omega_0}\right)^2 + g_a\left(\frac{\Omega}{\omega_0}\right)\right] \tag{16}$$

Solving Eq. (16) for Ω,[13,18]

$$\frac{\Omega}{\omega_0} = (\alpha + i\omega)/\omega_0 = \left[\left(-\frac{g_a}{2}\right) + \psi\right] + i\left(\frac{k_I}{2\psi}\right) \tag{17}$$

where

$$\psi = \pm\left(\frac{1}{\sqrt{2}}\left\{\sqrt{\left[\left(\frac{g_a}{2}\right)^2 - k_R\right]^2 + k_I^2} + \left[\left(\frac{g_a}{2}\right)^2 - k_R\right]\right\}^{1/2}\right)$$

By routine algebraic manipulations, the instability is seen to occur when $g_a = k_I/k_R$[12,13] and the corresponding limit cycle frequency value is $(\omega/\omega_0) = \sqrt{k_R}$. However, this instability is not catastrophic, as the panel response does not grow indefinitely but rather a limit cycle oscillation is developed with increasing amplitude as λ increases. The value of g_a can be correlated with the equivalent term of the first approach (μ/M_∞), and one can write it for the same response parameters as

$$g_a^2 = \lambda\left(\frac{\mu}{M_\infty}\right) \tag{18}$$

As a typical example, a hinged-hinged panel with an amplitude value of $(a/h = 0.6)$ is considered by the second approach, and the eigenvalues k_1 and k_2 vs λ are plotted in Fig. 3, referred to as case b. Corresponding values of Ref. 13 are also plotted in Fig. 3. While the first eigenvalues k_1 of Ref. 13 have almost coincided with the two approaches up to $\lambda < 300$, the second eigenvalues k_2 are found to be more than the present ones. The reason for this appears to be that the reference amplitude value is specified on the first two mode shapes independently and proceeded with the nonlinear analysis. The graph is made for the first eigenvalue when (a/h) is specified on the first mode and the second eigenvalue when (a/h) is specified on the second mode vs λ. It may be noted here that the reference amplitude specified on the first mode increases the second eigenvalue and vice versa, as the two are coupled nonlinearly, i.e., through N_x. Since coalescence of eigenvalues is sought as a critical condition, it is just sufficient to specify the amplitude value on the first mode alone, as in the present case.

The eigenvalues k_1 and k_2 of the preceding example are analyzed for the panel response parameters α and ω with aerodynamic damping $g_a = 0$, 10 and are plotted against λ in Fig. 4. The graph for α vs λ is seen to be parabolic in this case. The critical dynamic pressure value λ_{cr} has increased with aerodynamic damping, whereas the frequency value has reduced with damping, as expected.

In Fig. 5, the change of mode shape with λ for a hinged-hinged panel (case b) is shown. For $\lambda = 0$, the mode shape is a standing wave-type, and for $\lambda = 476.0$, it is a traveling wave-type. Although the mode shape remained a standing wave-type for $\lambda < 400.0$, the position of maximum amplitude shifted from $x/L = 0.5$ to $x/L = 0.75$ as λ approached a value of 400.0. This shift increased the value of N_x, as given in Eq. (8).

Numerical Results and Discussions

Various numerical examples with hinged-hinged, clamped-clamped, clamped-hinged, and hinged-clamped boundaries and immovable end conditions have been worked out using the two approaches suggested. While an eight-element idealization of the panel is used in the first approach, 12 elements are considered in the second approach. In Table 1, the linear frequency values, linear critical dynamic pressure, and linear flutter frequency values are given for the two idealizations considered. Their agreement with exact values is excellent, even for eight-element idealization.

In Table 2, the nonlinear frequency and the stretching force value at different amplitudes are presented. The

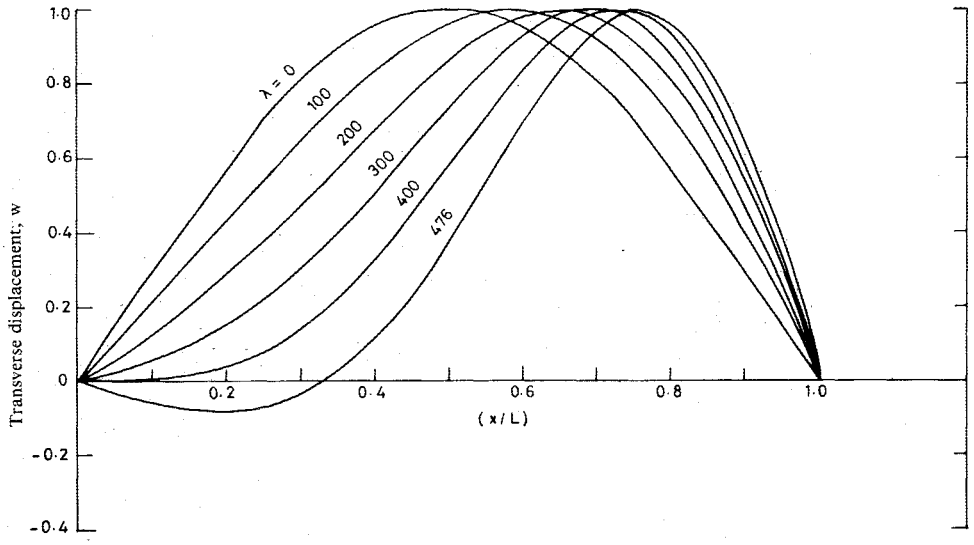

Fig. 5 Change of mode shape with dynamic pressure, hinged-hinged panel; $(a/h) = 0.6$; $= 0.33$ case b.

Table 1 Linear frequency and flutter coalescence values

Number of elements	In vacuo		Coalescence values	
	k_1	k_2	λ	k_{cr}
a) Hinged-hinged panel:				
8	97.409	1558.5	343.36	1051.8
12	97.409	1558.5	343.3573	1051.807
Exact[11]	97.4091	1558.55	343.3564	1051.797
b) Clamped-clamped panel:				
8	500.564	3803.5	636.5696	2741.4
12	500.56	3803.5	636.5691	2740.84
Exact[11]	500.564	3803.5	636.5691	2741.36
c) Hinged-clamped panel:				
8	237.72	2496.5	479.5637	1746.8
12	237.72	2496.5	479.568	1746.8

Table 2 Nonlinear frequency and stretching force values

Amplitude/ radius gyration	Hinged-hinged panel					Clamped-clamped panel			
	$(\omega/\omega_0)^2$			N_xL^2/EI		$(\omega/\omega_0)^2$		N_xL^2/EI	
	Exact[a,23]	FEM[b]	Present	Exact	Present	GFEM[20]	Present	GFEM[20]	Present
0.40	1.0400	1.0298	1.0400	0.3948	0.3948	1.0096	1.0096	0.3902	0.3902
0.80	1.1600	1.1189	1.1600	1.5791	1.5791	1.0383	1.0383	1.5607	1.5609
1.00	1.2500	1.1857	1.2500	2.4674	2.4674	1.0598	1.0598	2.4384	2.4381
2.00	2.0000	1.7379	2.0000	9.8696	9.8696	1.2381	1.2382	9.7460	9.7452
3.00	3.2500	2.6439	3.2500	22.206	22.206	1.5319	1.5320	21.9099	21.9087
4.00	5.0000	3.8869	5.0000	39.478	39.478	1.9376	1.9377	38.9286	38.9286

[a]Connotation for ω^2 as $\ddot{w} = -\omega^2 w$ is used. [b]Values from Ref. 14 to Ref. 17.

nonlinear frequency values in the case of a hinged-hinged panel are compared with Ref. 23, which gives a classical solution, and by the connotation for ω^2, as $\ddot{W} = -\omega^2 w$ is used. In the case of clamped-clamped panels, the comparison is made with Ref. 20, where Galerkins' finite-element approach is used. Other FEM results presented therein show a lower hardening behavior, and the reasons for this have been discussed in Ref. 17.

The nonlinear phenomenon is mainly governed by the nonlinear stretching force. A typical case with amplitude $(a/h = 0.40)$ and $\lambda = 396.0$ is taken, and the solution by the second approach is obtained using the linear vibration and linear panel flutter modes as the two starting solutions. The change of N_x value during the iteration is given in Table 3a. In Table 3b values of $N_xL^2(1-\nu^2)/EI$ obtained by the two approaches are presented for all amplitude values. In the first approach, N_x is calculated for $\lambda = 0$ and maintained constant for all λ values during nonlinear panel flutter solution, whereas in the second approach, N_x is given at $\lambda = \lambda_{cr}$ by updating N_x at each iteration. It may be noted here that the N_x value obtained by the first approach has been lower than that obtained by the second approach, and therefore,

Table 3a Change of nonlinear stretching force $(N_x L^2/EI)(1-\nu^2)$ with iterations hinged-hinged panel, $a/t=0.40$, $\lambda=396.0$

Iteration number	1	2	3	4	5	6	Eigenvalues k_1	k_2
Linear free vibration solution	4.31104	6.9979	6.6961	6.7998	6.7584	—	1184.5	1365.7
Linear panel flutter solution	6.9545	6.7084	6.7939	6.7604	6.7729	6.7681	1183.2	1367.5

Table 3b Value of nonlinear stretching force $[N_x L^2/EI(1-2)^2]$ for various amplitude values, hinged-hinged panel

a/h	0.1	0.2	0.4	0.6	0.8	1.00
First approach	0.2694	1.0777	4.3110	9.6998	17.2442	26.9440
Second approach	0.4348	1.7413	7.0022	15.9278	28.8617	46.5486
	(346.8)[a]	(357.5)	(401.0)	(476.0)	(591.0)	(751.0)

[a]corresponding λ values.

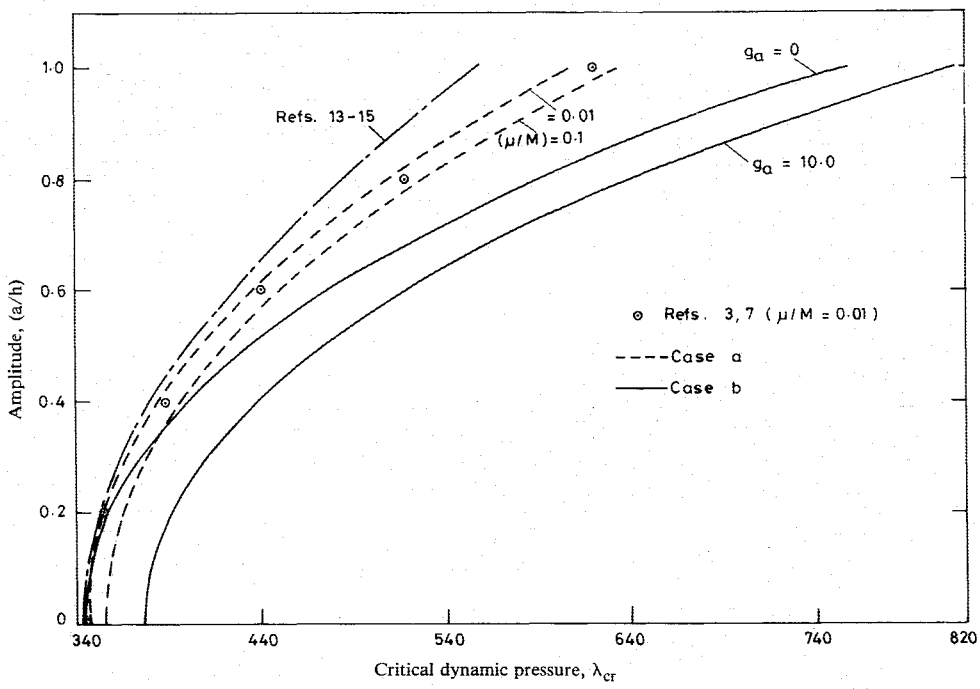

Fig. 6 Limit cycle amplitude vs critical dynamic pressure, hinged-hinged panel.

the critical dynamic pressure obtained by the second approach has been higher than that obtained by the first approach.

In Figs. 6–8, the amplitude (a/t) vs critical dynamic pressure λ_{cr} curves are given for all sets of boundary conditions. Curves showing the effect of aerodynamic damping on λ_{cr} for $\mu/M_\infty=0.01$, 0.1 in case a and $g_a=0$, 10 in case b are also given. In Fig. 6, the graph for a hinged-hinged panel—case a, $\mu/M_\infty=0.01$—is compared with Refs. 3 and 7 and shows close agreement. The curves given for case b show higher critical dynamic pressure. The curves based on the finite-element analysis of Refs. 13 and 15 are also given in Fig. 6. It can be seen that the critical dynamic pressure obtained in Refs. 13 and 15 is lower than that of case b, although a similar solution approach is made use of in their analysis, and they are also lower than case a results. This discrepancy can be attributed to the approximations used in modeling nonlinear effects in Refs. 13 and 15, as discussed in Ref. 17. In determining λ_{cr} values by the second approach, we have faced some difficulty in getting the converged eigenvalue as λ approached λ_{cr} (very close to the instability point) at higher amplitudes. This problem is overcome by obtaining the eigenvalues for $\lambda>\lambda_{cr}$ where the roots are complex conjugate pairs and the instability point is identified from the response parameter α vs λ, when α changes its sign from negative to positive.[2,18]

In Figs. 7 and 8, amplitude vs critical dynamic pressure curves for clamped-clamped, clamped-hinged, and hinged-clamped panels with different aerodynamic clamping values are given, and are compared with those of Ref. 15. One interesting observation here is that λ_{cr} remains the same for hinged-clamped and clamped-hinged panels at all amplitude levels for case a, whereas in case b, λ_{cr} has been different for the two sets of boundary conditions,[15] as expected.

In Tables 4–7, the changes in mode shapes at different amplitude values and at the corresponding λ_{cr} values for all boundary conditions are presented. Even though the starting solution has been a standing wave-type for case a, it changed into a traveling wave-type when λ reached λ_{cr} at all amplitude levels. With the increase in amplitude level, the deflection of the mode shape has decreased in the region $0<x<0.75L$ for both hinged-hinged and clamped-clamped panels. In Tables 6 and 7, the mode shapes are presented for clamped-hinged and hinged-clamped panels. The mode shape

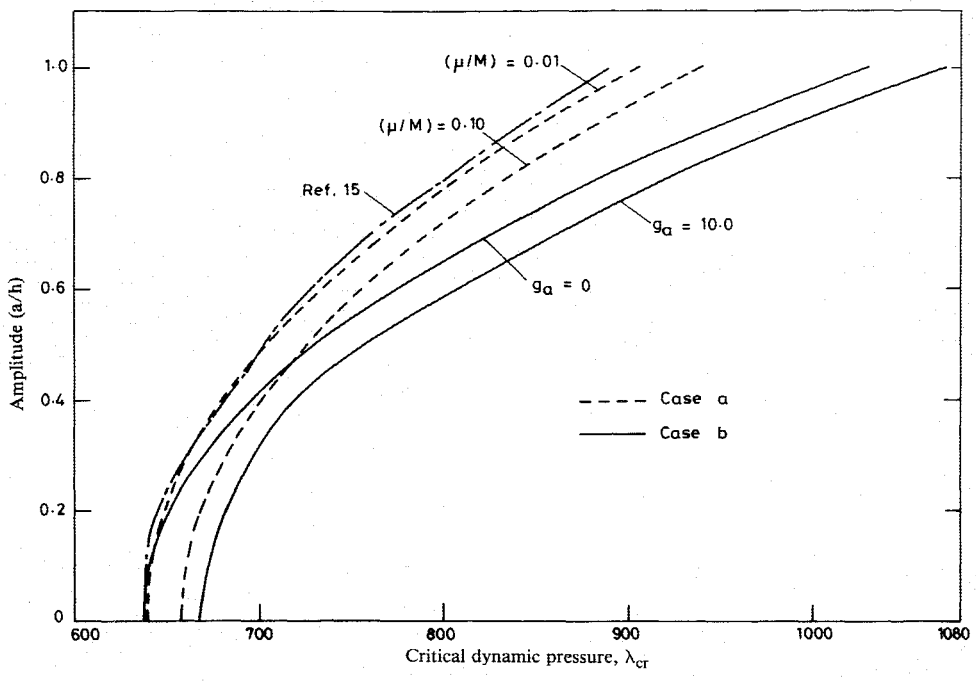

Fig. 7 Limit cycle amplitude vs critical dynamic pressure, clamped-clamped panel.

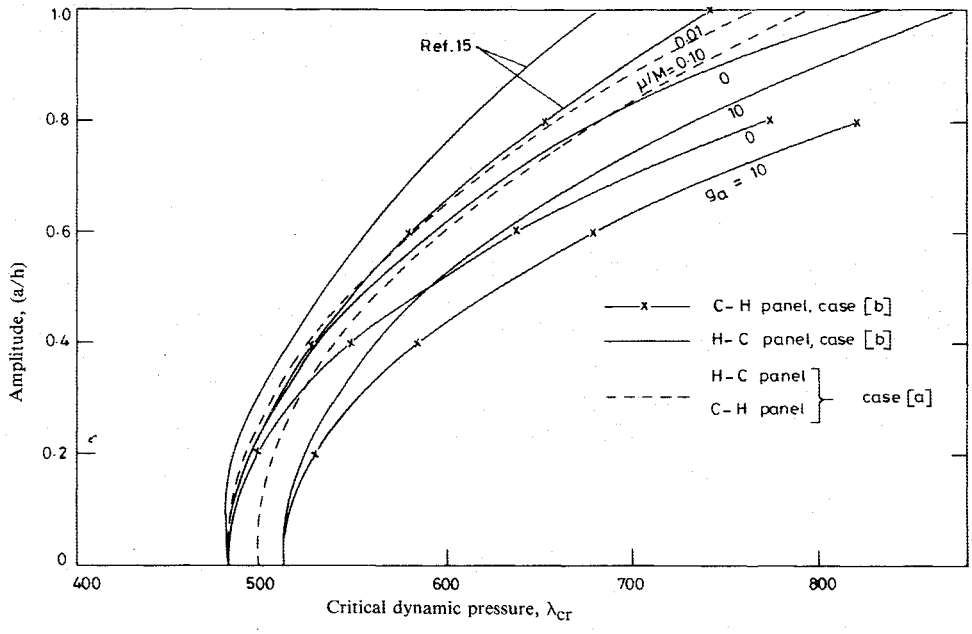

Fig. 8 Limit cycle amplitude vs critical dynamic pressure, hinged-clamped and clamped-hinged panels.

Table 4 Change of normalized mode shapes with amplitude for hinged-hinged panels

	$a/h=0.0$	0.20	0.40	0.60	0.80	1.00
x/L	$\lambda=0.0$	353.5	383.0	433.0	506.0	603.5
			Case a			
0.0	0.0	0.0	0.0	0.0	0.0	0.0
0.125	0.3826	−0.0800	−0.0762	−0.0704	−0.0632	−0.0553
0.250	0.7071	−0.0838	−0.0805	−0.0756	−0.0693	−0.0624
0.500	1.0000	0.4092	0.4011	0.3885	0.3720	0.3528
0.750	0.3827	0.7319	0.7375	0.7467	0.7594	0.7753
1.000	0.0	0.0	0.0	0.0	0.0	0.0
			Case b			
	$a/h=0.0$	0.20	0.40	0.60	0.80	1.00
x/L	$\lambda=343.3$	357.5	401.0	476.0	591.0	757.0
0.0	0.0	0.0	0.0	0.0	0.0	0.0
0.16667	−0.0959	−0.0937	−0.0876	−0.0786	−0.0677	−0.0560
0.2500	−0.0850	−0.0833	−0.0786	−0.0717	−0.0632	−0.0539
0.5000	0.4121	0.4081	0.3964	0.3785	0.3551	0.3276
0.7500	1.0000	1.0000	1.0000	1.0000	1.0000	1.0000
1.0000	0.0	0.0	0.0	0.0	0.0	0.0

Table 5 Change of normalized mode shapes with amplitude for clamped-clamped panel

x/L	$a/h=0.20$		0.40		0.60		0.80		1.00	
	$\lambda=0.0$	647.0	0.0	677.5	0.0	730.0	0.0	805.0	0.0	905.0
					Case a					
0.0	0.0	0.0	0.0	0.0	0.0	0.0	0.0	0.0	0.0	0.0
0.125	0.1788	−0.0514	0.1805	−0.0495	0.1841	−0.0464	0.1887	−0.0425	0.1942	−0.0382
0.250	0.5449	−0.0997	0.5474	−0.0964	0.5519	−0.0910	0.5578	−0.0843	0.5647	−0.0766
0.500	1.0000	0.4333	1.0000	0.4258	1.0000	0.4136	1.0000	0.3977	1.0000	0.3788
0.750	0.5445	1.0000	0.5474	1.0000	0.5519	1.0000	0.5578	1.0000	0.5647	1.0000
1.000	0.0	0.0	0.0	0.0	0.0	0.0	0.0	0.0	0.0	0.0

Case b

x/L	$a/h=0.0$	0.20	0.40	0.60	0.80	1.00
	$\lambda=636.6$	652.0	697.5	774.0	884.0	1030.8
0.0	0.0	0.0	0.0	0.0	0.0	0.0
0.16667	−0.0776	−0.0762	−0.0721	−0.0660	−0.0587	−0.0508
0.250	−0.1009	−0.0992	−0.0943	−0.0870	−0.0781	−0.0685
0.500	0.4359	0.4321	0.4210	0.4041	0.3827	0.3581
0.750	0.9998	1.0000	1.0000	1.0000	1.0000	1.0000
1.00	0.0	0.0	0.0	0.0	0.0	0.0

Table 6 Change of normalized mode shapes with amplitude for clamped-hinged panel

x/L	$a/h=0.20$		0.40		0.60		0.80		1.00	
	$\lambda=0.0$	490.0	0.0	522.0	0.0	576.0	0.0	655.0	0.0	761.5
					Case a					
0.0	0.0	0.0	0.0	0.0	0.0	0.0	0.0	0.0	0.0	0.0
0.125	0.1368	−0.0499	0.1411	−0.0475	0.1478	−0.0439	0.1563	−0.0395	0.1661	−0.0347
0.250	0.4397	−0.1229	0.4485	−0.1170	−0.4620	−0.1082	0.4785	−0.0975	0.4967	−0.0860
0.500	0.9718	0.2045	0.9764	0.2052	0.9832	0.2055	0.9913	0.2046	0.9998	0.2021
0.750	0.8192	1.0000	0.8165	1.0000	0.8127	1.0000	0.8082	1.0000	0.8037	1.0000
1.00	0.0	0.0	0.0	0.0	0.0	0.0	0.0	0.0	0.0	0.0

Case b

x/L	$a/h=0.0$	0.20	0.40	0.60	0.80	1.00
	$\lambda=479.6$	497.0	549.0	639.0	777.0	978.0
0.0	0.0	0.0	0.0	0.0	0.0	0.0
0.16667	−0.0794	−0.0772	−0.0715	−0.0633	−0.0536	−0.0435
0.250	−0.1125	−0.1215	−0.1124	−0.0995	−0.0845	−0.0690
0.500	0.2042	0.2045	0.2054	0.2049	0.2017	0.1948
0.750	1.0000	1.0000	1.0000	1.0000	1.0000	1.0000
1.00	0.0	0.0	0.0	0.0	0.0	0.0

Table 7 Change of normalized mode shapes with amplitude for hinged-clamped panel

x/L	$a/h=0.20$		0.40		0.60		0.80		1.00	
	$\lambda=0.0$	490.0	0.0	522.0	0.0	576.0	0.0	655.0	0.0	761.5
					Case a					
0.0	0.0	0.0	0.0	0.0	0.0	0.0	0.0	0.0	0.0	0.0
0.125	0.4604	−0.0647	0.4581	−0.0637	0.4546	−0.0618	0.4507	−0.0581	0.4468	−0.0523
0.250	0.8192	−0.0197	0.8165	−0.0222	0.8127	−0.0254	0.8082	−0.0283	0.8037	−0.0297
0.500	0.9718	0.6499	0.9764	0.6401	0.9832	0.6249	0.9913	0.5977	0.9998	0.5557
0.750	0.4397	0.9503	0.4485	0.9632	0.4620	0.9841	0.4785	1.0000	0.4967	1.0000
1.000	0.0	0.0	0.0	0.0	0.0	0.0	0.0	0.0	0.0	0.0

Case b

x/L	$a/h=0.0$	0.20	0.40	0.60	0.80	1.00
	$\lambda=479.6$	492.0	529.0	594.0	694.0	839.0
0.0	0.0	0.0	0.0	0.0	0.0	0.0
0.16667	−0.0654	−0.0651	−0.0643	−0.0625	−0.0590	−0.0539
0.250	−0.0181	−0.0190	−0.0216	−0.0249	−0.0278	−0.0295
0.500	0.6285	0.6335	0.6095	0.5873	0.5582	0.5236
0.750	0.9100	0.9133	0.9227	0.9382	0.9603	0.9889
1.00	0.0	0.0	0.0	0.0	0.0	0.0

is seen to flatten out in the negative side as well as up to the maximum positive deflection. The deflections then increase up to the support end at all amplitude values. Although the critical dynamic pressure value has been the same for hinged-clamped and clamped-hinged panels for case a, the mode shapes have been quite different. In case b, λ_{cr} as well as the mode shapes have been different.

Conclusions

The effectiveness of the finite-element formulation in the study of nonlinear panel flutter is demonstrated here. Two solution techniques are presented. In the first method, the nonlinear vibration problem is solved assuming that linear vibration mode, and the nonlinear panel flutter solution is obtained by adding the aerodynamic force matrix for these nonlinear matrices and iterating them for flutter coalescence. In the second approach, the solution of the linear panel flutter is made use of for solving the nonlinear panel flutter, and iterations are made for flutter coalescence. The second approach has shown an increased hardening effect, and hence, critical dynamic pressure is greater than that obtained by the first approach at all limit cycle amplitudes. Results based on the second approach can be considered to be an improvement over the first one, because the nonlinear stretching forces also iterated, along with flutter equations.

The effect of aerodynamic damping is introduced, based on the two simplifications available in literature, and a relation between these two representations is derived. The response parameters of the panel are calculated. The effect of aerodynamic damping is shown to increase the critical dynamic pressure. The changes in mode shapes with increases in amplitude have been significant for clamped-clamped, clamped-hinged, and hinged-clamped panels.

Current results are compared with the available analytical and finite-element method solutions. It is believed that these formulation and solution techniques will be useful in the investigation of nonlinear panel flutter of thin/thick plates and cylindrical shells.

Acknowledgment

The first author is grateful to the Director, Defence Research and Development Laboratory, Hyderabad, for giving permission to pursue this research topic as part of his research program at IIT Madras.

References

[1]Dowell, E. H., "Panel Flutter: A Review of the Aeroelastic Stability of Plates and Shells, *AIAA Journal*, Vol. 8, March 1970, pp. 385-399.

[2]Dugundji, J., "Theoretical Considerations of Panel Flutter at High Supersonic Mach Numbers," *AIAA Journal*, Vol. 4, July 1986, pp. 1257-1266.

[3]Dowell, E. H., "Nonlinear Oscillations of a Fluttering Plate," *AIAA Journal*, Vol. 4, July 1966, pp. 1267-1275.

[4]Dowell, E. H., "Nonlinear Oscillations of a Fluttering Plate II," *AIAA Journal*, Vol. 5, Oct. 1967, pp. 1856-1862.

[5]Olson, M. D. and Fung, Y. C., "Comparing Theory and Experiment for the Supersonic Flutter of Circular Cylindrical Shells," *AIAA Journal*, Vol. 5, Oct. 1967, pp. 1849-1855.

[6]Morino, L., "A Perturbation Method for Treating Nonlinear Panel Flutter Problems," *AIAA Journal*, Vol. 7, March 1969, pp. 405-411.

[7]Kuo, C.-C., Morino, L., and Dugundji, J., "Perturbation and Harmonic Balance Method for Nonlinear Panel Flutter," *AIAA Journal*, Vol. 10, Nov. 1972, pp. 1479-1484.

[8]Kobayashi, S., "Flutter of Simply Supported Rectangular Panels in a Supersonic Flow—Two-Dimensional Panel Flutter—Simply Supported Panels II—Clamped Panels," *Transactions of Japan Society for Aeronautical and Space Sciences*, Vol. 8, 1962, pp. 79-118.

[9]Bolotin, V. V., *Nonconservative Problems of the Theory and Elastic Stability*, Macmillan, New York, 1963, pp. 274-312.

[10]Esten, F. E. and McIntosh, S. S., "Analysis of Nonlinear Panel Flutter and Response under Random Excitation or Nonlinear Aerodynamic Loading," *AIAA Journal*, Vol. 9, March 1971, pp. 411-418.

[11]Olson, M. D., "On Applying Finite Elements to Panel Flutter," LR-476, National Research Council, Ottawa, Canada, March 1967.

[12]Sander, G., Bon, C., and Geradin, M., "Finite Element Analysis of Supersonic Panel Flutter," *International Journal of Numerical Methods in Engineering*, Vol. 7, 1973, pp. 379-394.

[13]Chuh Mei, "A Finite Element Approach for Nonlinear Panel Flutter," *AIAA Journal*, Vol. 15, Aug. 1977, pp. 1107-1110.

[14]Mei, C. and Rogers, J. L., Jr., "NASTRAN—Nonlinear Vibration Analysis of Beams and Frame Structures," NASA TMX-3278, 1975, pp. 259-284.

[15]Singa Rao, K. and Venkateswara Rao, G., "Large Amplitude Supersonic Flutter of Panels with Ends Elastically Restrained Against Rotation," *Computers and Structures*, Vol. 11, 1980, pp. 197-201.

[16]Prathap, G., "Comments on a Finite Element Approach for Nonlinear Panel Flutter," *AIAA Journal*, Vol. 16, Aug. 1978, pp. 863-864.

[17]Sarma, B. S. and Varadan, T. K., "Certain Discussions in the Finite Element Formulations of Nonlinear Vibration Analysis," *Computers and Structures*, Vol. 15, 1982, pp. 643-646.

[18]Bisplinghoff, R. L., "Principles of Aeroelasticity," Wiley, New York, 1962.

[19]Sarma, B. S. and Varadan, T. K., "Lagrange-Type Formulation for Finite Element Analysis of Nonlinear Beam Vibration," *Journal of Sound and Vibration*, Vol. 86, 1983, pp. 61-70.

[20]Bhashyam, G. R. and Prathap, G., "Galerkin Finite Element Method for Nonlinear Beam Vibrations," *Journal of Sound and Vibration*, Vol. 72, 1980, pp. 191-203.

[21]Bergan, P. G. and Clough, R. W., "Convergence Criteria for Iterative Processes," *AIAA Journal*, Vol. 10, Aug. 1972, pp. 1107-1108.

[22]Voss, H. M. and Dowell, E. H., "Effect of Aerodynamic Damping on Flutter of Thin Panels," *AIAA Journal*, Vol. 2, Jan. 1964, pp. 119-120.

[23]Woinowsky-Krieger, S., "The Effect of an Axial Force on the Vibration of Hinged Bars," *Journal of Applied Mechanics*, Vol. 17, 1950, pp. 35-36.